



Cite this: *React. Chem. Eng.*, 2025, 10, 2991

## Copper-based metal-organic frameworks as highly efficient catalysts for the biomimetic catalytic synthesis of theaflavins

Shaolong Du,<sup>a</sup> \*<sup>ab</sup> Zhimei Zhou,<sup>b</sup> Zetao Du<sup>c</sup> and Junyi Chang<sup>a</sup>

Theaflavins (TFs) are the principal quality and active compounds present in fermented tea, generated during the fermentation process. Due to the exceedingly low concentration of TFs in black tea, the *in vitro* synthesis of TFs has emerged as a predominant trend in industrial production. Despite significant advancements in the *in vitro* research of TFs in recent years, several challenges remain in the preparation of TFs according to established literature methods. These challenges include the high cost of natural enzyme preparation, difficulties in preservation, and poor thermal and chemical stability. Consequently, the development of efficient and stable catalysts has emerged as a critical issue for the industrial preparation of TFs. This study investigated the feasibility of utilizing Cu-BTC (copper(II) benzene-1,3,5-tricarboxylate) metal-organic frameworks (MOFs) as biomimetic catalysts for the synthesis of TFs from catechins. Cu-BTC was synthesized using a solvothermal method and characterized. The synthesized Cu-BTC exhibited an octahedral structure and demonstrated commendable thermal stability. The enzyme-like activity of Cu-BTC was evaluated using catechol as the substrate, yielding kinetic parameters of  $V_{max} = 0.0338 \text{ mM s}^{-1}$  and  $K_m = 14.19 \text{ mM}$ , which indicated substantial polyphenol oxidase-like catalytic activity. Cu-BTC was employed to catalyze the oxidation of catechins to synthesize TFs. The results indicated that the total yield of catechins using Cu-BTC as a biomimetic catalyst was 30% higher than that achieved through chemical oxidation methods and 50% higher than that of tyrosinase. The optimal catalytic reaction conditions were determined as follows: a reaction temperature of 80 °C, a reaction time of 60 minutes, a pH of 5.0, and a Cu-BTC dosage of 0.05 g mL<sup>-1</sup>, resulting in a total yield of TFs of 800 µg mL<sup>-1</sup>. This study verified that the copper-based MOF Cu-BTC was not only facile to prepare, but also exhibited excellent catalytic activity and thermal stability, which opens promising prospects for the development of new biomimetic catalysts for the synthesis of TFs.

Received 15th June 2025,  
Accepted 20th August 2025

DOI: 10.1039/d5re00261c  
[rsc.li/reaction-engineering](http://rsc.li/reaction-engineering)

## 1. Introduction

Theaflavins (TFs) are polyphenolic pigments found in black tea, characterized by their unique benzotropolone structure (see Fig. 1).<sup>1</sup> These compounds are formed through the oxidative polymerization of catechins, a process that is catalysed by polyphenol oxidase (PPO) during the fermentation of black tea.<sup>2</sup> TFs are considered key quality components that directly influence the colour and flavour of black tea.<sup>3</sup> Pharmacological studies have demonstrated that TFs exhibit a range of health benefits and pharmacological functions, including antioxidant, antibacterial, and antiviral properties, as well as roles in cancer prevention and treatment, and the prevention of cardiovascular diseases.<sup>4–6</sup> However, the concentration of TFs in black tea is notably low

(less than 1%); researchers have attempted to synthesize TFs using *in vitro* enzymatic oxidation methods, achieving significant advancements in both yields and product purity.<sup>7</sup>

Polyphenol oxidase (PPO) is a type of copper-binding enzyme widely found in plants and microorganisms, including tea leaves.<sup>8</sup> It catalyses the oxidation of polyphenols, such as catechins, into quinones and serves as

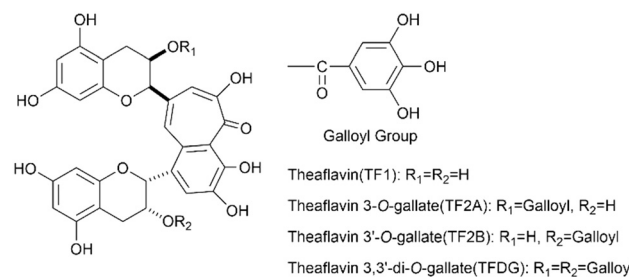


Fig. 1 Chemical structure of the four main theaflavins.

<sup>a</sup> College of Chemical Engineering and Chemistry, Hunan Normal University, Changsha 410081, China. E-mail: dsl@hunnu.edu.cn

<sup>b</sup> Hunan Xinsheng Tea Science and Technology Co., Ltd., Shaoyang, 422900, China

<sup>c</sup> School of Management, Fudan University, Shanghai 200433, China



a key enzymatic catalyst in the oxidative polymerization of catechins to form TFs.<sup>9</sup> Polyphenol oxidase (PPO) exhibits several advantages, including high catalytic activity, substrate specificity, and the ability to operate under mild reaction conditions. However, challenges associated with the purification of natural PPO, difficulties in preservation, and the presence of numerous activity inhibitors contribute to elevated costs in obtaining natural PPO.<sup>10</sup> These issues hinder the industrial realization of enzymatic oxidative synthesis of TFs. Therefore, it is necessary to develop enzyme substitute catalysts with low cost and stable properties.

Metal-organic frameworks (MOFs) are a novel category of porous coordination crystal materials formed through the bonding of metal ions (or metal clusters) with organic ligands *via* coordination bonds.<sup>11</sup> Their distinctive physical and chemical characteristics, including high porosity, tunable void structures, and convenient surface functionalization, have led to extensive applications in fields such as catalytic reactions, adsorption separation, and sensor development. Recently, both MOFs and their composite materials have showcased outstanding enzyme-mimicking abilities. As a new type of enzyme mimic, MOFs not only demonstrate catalytic activities comparable to those of natural enzymes, but also present notable benefits regarding stability, production costs, and structural variety.<sup>12</sup> As a result, they are viewed as highly promising alternatives to natural enzymes. Yang *et al.*<sup>13</sup> created CeO<sub>2</sub> metal-organic framework (CeO<sub>2</sub>-MOF) nanorods through hydrothermal and calcination methods, revealing exceptional nanozyme catalytic capabilities for antibacterial applications. Furthermore, the CeO<sub>2</sub>-MOF exhibited impressive stability and could be reused effectively. Yang *et al.*<sup>14</sup> synthesized a bismuth metal-organic framework nanozyme (BiO-BDC-NH<sub>2</sub>) and developed a colorimetric technique for the detection of Cr<sup>6+</sup>, achieving a detection limit of 0.44 ng mL<sup>-1</sup>, based on the principle that Cr<sup>6+</sup> enhances the peroxidase-like activity of the BiO-BDC-NH<sub>2</sub> nanozyme. Xiong *et al.*<sup>15</sup> utilized a simple self-assembly process to construct an amorphous zeolitic imidazolate framework (aZIF), which demonstrated a 2.2-fold enhancement in CA-like hydrolytic activity when compared to crystalline ZIFs. Singh *et al.*<sup>16</sup> investigated the dependence of oxidase activity and specificity on the thickness of Cu-MOF nanosheets. Notable differences in oxidase activity were found among Cu-MOFs of varying thicknesses. The ultrathin (4 nm) Cu-UMOF demonstrated high efficiency and specificity for catechol oxidation, whereas the thicker Cu-MOF nanosheets (20–30 nm) exhibited diminished catechol oxidase and peroxidase activities. Although there have been no reports on the application of MOFs in the synthesis of theaflavins through the oxidation of catechins, the aforementioned studies have inspired us to synthesize Cu-MOFs and utilize them as substitutes for PPO in catalysing the oxidative polymerization of catechins.

In this study, we first synthesized Cu-MOFs using the hydrothermal method and characterized their structure through scanning electron microscopy (SEM), Fourier-

transform infrared spectroscopy (FTIR), and X-ray diffraction spectroscopy (XRDS). Subsequently, we tested the PPO-like enzyme activity of Cu-MOFs using catechol as the substrate. Finally, Cu-MOFs were applied to the oxidative polymerization of catechins to synthesize theaflavins. The results demonstrated that Cu-MOFs not only efficiently catalysed the oxidative polymerization of catechins to synthesize theaflavins, but also exhibited excellent substrate selectivity, with the yield of TF1 being significantly higher than that of the other three main theaflavin monomers.

## 2. Materials and methods

### 2.1 Materials

Benzene-1,3,5-tricarboxylic acid (H<sub>3</sub>BTC) was purchased from Shanghai Bide Pharmatech Ltd. Cu(NO<sub>3</sub>)<sub>2</sub>·3H<sub>2</sub>O was purchased from Shandong Keyuan Biochemical Co., Ltd. The four main theaflavin standards (TF1, TF2A, TF2B, and TFDG, 98%) were obtained from Shanghai Yuanye Bio-Technology Co., Ltd. Additionally, the four primary catechin standards (EC, EGC, ECG, and EGCG, 95%) were sourced from Shanghai Macklin Biochemical Technology Co., Ltd. The model catechin extracts, with a total catechin purity of 92.35%, consisting of 22.63% EGC, 21.25% EC, 20.15% ECG, and 28.32% EGCG, were provided by Hunan A-plus Biotechnology Co., Ltd. All other reagents used in this study were of analytical grade and did not require further purification.

### 2.2 Synthesis of the copper-based metal-organic framework (Cu-BTC)

Cu-BTC was synthesized using a hydrothermal technique as previously reported by Ibrahim.<sup>17</sup> A total of 2.14 mmol (0.45 g) of benzene-1,3,5-tricarboxylic acid (H<sub>3</sub>BTC) was stirred in 48 mL of anhydrous ethanol for 10 minutes. Subsequently, 3.1 mmol (2.49 g) of copper nitrate trihydrate (Cu(NO<sub>3</sub>)<sub>2</sub>·3H<sub>2</sub>O) was added to the solution, and stirring was continued for an additional 60 minutes. The resulting solution was then transferred into a 100 mL PTFE-lined stainless-steel autoclave and subjected to a reaction at 120 °C for 24 h. Upon completion of the reaction, the mixture was allowed to cool to room temperature naturally. Finally, the resulting MOFs were washed three times with anhydrous ethanol, centrifuged, and placed in a vacuum drying oven, where it was dried at 60 °C for 12 hours.

### 2.3 Characterization of Cu-BTC

Cu-BTC MOFs were characterized using different techniques. The X-ray diffraction (XRD) patterns were recorded on a D8 Advance powder X-ray diffractometer (Bruker, Germany) equipped with Cu K $\alpha$  radiation in the  $2\theta$  range from 5° to 35° at 40 kV and 40 mA. The scanning electron microscopy (SEM) images were recorded on a JEM-2100F microscope (FEI, USA). Thermogravimetric analysis (TGA) was carried out under an air atmosphere using a STA 409 PC DTA TG thermal analyzer

(Netzsch, Germany) at a heating rate of 10 K min<sup>-1</sup>. The infrared spectrum was measured using an AVATAR370 Fourier transform infrared spectrometer (Nicolet, USA) in the wavenumber range of 500–4000 cm<sup>-1</sup> to detect functional groups.

#### 2.4 Determination of enzyme activity

The enzyme activity of Cu-BTC was assessed using colorimetric methods, following the approach outlined by Zhan<sup>18</sup> with slight modifications. In a quartz cuvette, 1.0 mL of phosphate buffer (pH 6.5) and 1.0 mL of 0.6 mol L<sup>-1</sup> pyrocatechol solution were combined. After allowing capillary bubbling at room temperature for 4 to 5 minutes, 1.0 mL of a 0.01 g mL<sup>-1</sup> Cu-BTC solution was introduced. The cuvette was subsequently placed in an ultraviolet-visible spectrophotometer to dynamically measure the absorbance of the reaction system at a wavelength of 410 nm over a duration of 30 minutes. A curve was constructed to illustrate the changes in absorbance over time, facilitating the determination of Cu-BTC's activity under the specified conditions. The activity of the mimic enzyme was calculated using the following formula:

$$U = \frac{(A_1 - A_0)}{0.001 \times m \times t}$$

where,  $U$  represents the enzyme specific activity of PPO measured in units (U mg<sup>-1</sup>).  $A_0$  and  $A_1$  denote the absorbance values of the reaction system at initial and time  $t$ , respectively.  $m$  refers to the mass (in grams) of Cu-BTC added to the system, and  $t$  indicates the reaction time, measured in minutes (min).

#### 2.5 Catalytic synthesis of TFs using Cu-MOFs

Weigh 10 to 70 mg of Cu-MOFs and 0.1 g of model catechin extracts into a 50 mL EP tube. Add 10 mL of citrate-phosphate buffer (pH 3.0–8.0) and stir the mixture magnetically at 200 rpm in a water bath maintained at a temperature range of 60 to 90 °C, while exposing it to air for a duration of 15 to 90 minutes. Immediately after the reaction, place the reaction solution in an ice–water bath for 5 minutes to terminate the reaction. After cooling, add an equal volume of ethyl acetate to the solution and perform three extraction cycles. Use a plastic pipette to draw the upper layer of the extract and transfer it to a clean, dry round-bottom flask of appropriate size. Evaporate the extract to dryness using a rotary evaporator to obtain the theaflavin product. Finally, dissolve the product in 1 mL of deionized water to prepare a solution, and filter it through a 0.45 µm microporous membrane to obtain the sample solution.

#### 2.6 HPLC analysis of catechins and TFs

The catechin and TF levels of the reaction samples were measured by HPLC according to the method reported by Kong.<sup>19</sup> The supernatants of the aforementioned sample solutions were analyzed for TF constituents using high-

performance liquid chromatography (HPLC) with a Venusil MP C<sub>18</sub> column (4.6 mm i.d. × 250 mm, 5 µm) and an Agilent LC-1100 system (Santa Clara, USA). The eluate was monitored at a wavelength of 280 nm while maintaining a column temperature of 35 °C. The eluent comprised mobile phase A (acetonitrile) and mobile phase B (5 mmol L<sup>-1</sup> phosphate solution), with the gradient conditions detailed in Table 1. The solvent flow rate was set to 0.6 mL min<sup>-1</sup>, and the injection volume was 20 µL.

The absorption peaks of four catechins and theaflavins were identified based on the retention times of the corresponding standard compounds. The concentrations of catechins and theaflavins were calculated using the standard curves of the respective standard compounds and the measured peak areas of catechins and theaflavins.

#### 2.7 Catalytic synthesis of theaflavins by chemical oxidation

The catalytic oxidation of catechins to synthesize theaflavins was performed using chemical reagents as catalysts. Fe(NO<sub>3</sub>)<sub>3</sub>, FeCl<sub>3</sub>, Fe(SO<sub>4</sub>)<sub>3</sub>, and H<sub>2</sub>O<sub>2</sub> were selected as catalysts under acidic conditions, while KMnO<sub>4</sub> and NH<sub>4</sub>OH were chosen for reactions under alkaline conditions. The optimal reaction time, temperature, and pH conditions for the chemical oxidation method were referenced based on the relevant literature.<sup>20,21</sup>

Reaction conditions for alkaline oxidants: 40 mg of alkaline oxidants and 100 mg of catechins were dissolved in 10 mL of citrate–phosphate buffer and reacted under magnetic stirring. The reaction time was 45 minutes at a temperature of 45 °C, with a pH of 7.5.

Reaction conditions for acidic oxidants: 40 mg of acidic oxidant and 100 mg of catechins were dissolved in 10 mL of citric acid–phosphate buffer and reacted under magnetic stirring. The reaction lasted for 35 minutes at a temperature of 55 degrees Celsius and a pH of 5.5.

After the reaction was completed, the mixture was rapidly cooled to room temperature to terminate the reaction. An equal volume of ethyl acetate was added for extraction three times, and the concentration of theaflavins was determined using HPLC as described in section 2.6.

### 3. Results and discussion

#### 3.1 Structure and morphology characterization of Cu-BTC

To discern the structure and morphology of the catalyst, scanning electron microscopy (SEM) was conducted, as

**Table 1** Gradient elution procedures

t/min	Volume fraction of mobile phase/%	
	Mobile phase A	Mobile phase B
0	10	90
10	13	87
35	26	74
40	26	74
50	10	90



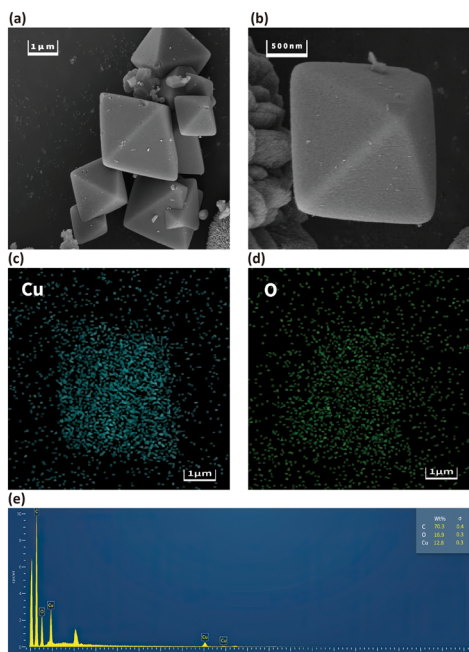


Fig. 2 (a) and (b) SEM images of the prepared Cu-BTC; (c) and (d) EDS mapping images of Cu and O in the prepared Cu-BTC; (e) EDS spectrum of the synthesized Cu-BTC.

illustrated in Fig. 2(a) and (b). The SEM images revealed that the prepared Cu-BTC exhibits excellent crystalline properties, characterized by a highly regular crystal morphology. The crystal surfaces are notably smooth, presenting a lipid-like appearance, and the material demonstrates preferential growth along specific crystallographic orientations. The material possesses a typical octahedral crystal configuration, with a uniform distribution of crystal sizes primarily ranging from 10 to 20  $\mu\text{m}$ , indicating good monodispersity. Additionally, elemental analysis (EDS) was performed to examine the elemental composition of Cu-BTC. The Cu-BTC structure, as depicted in Fig. 2(c)–(e), contained Cu, C, and O components, which were validated by the EDS spectra. Furthermore, Fig. 2(e) illustrates the elemental distribution of the MOF, showcasing the uniform dispersion of all constituent elements (Cu, C, and O) within the framework.

To further characterize the structural features of Cu-BTC, Fourier transform infrared spectroscopy (FTIR) was employed

for detailed analysis, with the results illustrated in Fig. 3(a). The infrared spectroscopy analysis revealed that the two absorption bands at  $1384\text{ cm}^{-1}$  and  $1635\text{ cm}^{-1}$  correspond to the symmetric and asymmetric stretching vibration modes of the carboxylate group ( $\text{COO}^-$ ), respectively. This characteristic confirms the successful coordination of the  $\text{H}_3\text{BTC}$  ligand. No significant characteristic absorption was detected in the region above  $1635\text{ cm}^{-1}$ , which fully demonstrates that the  $\text{H}_3\text{BTC}$  ligand achieved complete deprotonation in the reaction system, thereby providing strong evidence for efficient coordination between  $\text{Cu}^{2+}$  ions and the organic ligand. Additionally, the broad absorption band observed in the  $3000\text{--}3500\text{ cm}^{-1}$  range in the spectrum can be attributed to the stretching vibration characteristics of the O-H bond in water molecules adsorbed on the material's surface, indicating that the Cu-BTC material surface may exhibit certain hydrophilicity. Based on the comprehensive analysis of infrared spectroscopy, it can be confirmed that the  $\text{H}_3\text{BTC}$  ligand successfully formed the Cu-BTC metal-organic framework nanozyme with  $\text{Cu}^{2+}$  through coordination bonds. This result provides crucial information for subsequent research on its nanozyme catalytic performance. The characteristic peaks of the infrared spectrum are consistent with those reported in the literature for similar MOF materials, further verifying the successful synthesis of Cu-BTC and the reliability of its structure.

The bulk structure of the prepared Cu-BTC was analysed to investigate its composition and crystal structure. The X-ray diffraction (XRD) pattern of Cu-BTC, presented in Fig. 3(b), displays several distinct characteristic diffraction peaks within the  $2\theta$  range. These peaks exhibit high intensity and a narrow full width at half maximum, indicating the excellent crystallinity of the material. By analysing the narrow and intense diffraction peaks in the spectrum, it can be inferred that the prepared Cu-BTC possesses a large grain size, good crystallinity integrity, and high purity. These results demonstrate the successful synthesis of the highly crystalline metal-organic framework material Cu-BTC, providing a solid structural foundation for its catalytic applications.

The thermal stability of the synthesized Cu-BTC was examined using thermogravimetric analysis (TG). As illustrated in Fig. 3(c), the thermal decomposition of Cu-BTC can be categorized into two distinct mass loss stages. In the

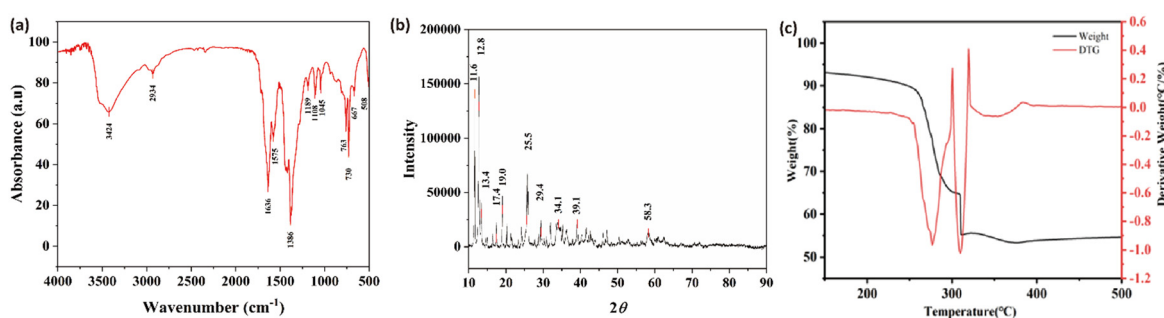


Fig. 3 (a) FT-IR spectrum; (b) XRD pattern; (c) TG graphs of the synthesized Cu-BTC.



initial stage, which ranges from room temperature to 250 °C, the mass loss is approximately 10%. This loss is primarily attributed to the evaporation of adsorbed water molecules and other solvent molecules present within the material. The gradual mass loss observed in this stage indicates that Cu-BTC maintains good structural stability under low-temperature conditions. As the temperature increases further, specifically within the range of 250–310 °C, a sharp decline in the mass of Cu-BTC is observed, accompanied by a significant increase in the rate of mass loss. This rapid loss is primarily due to the thermal decomposition of the organic ligands and the subsequent collapse of the metal-organic framework structure. In conclusion, Cu-BTC demonstrates excellent thermal stability up to 250 °C, which provides a critical theoretical foundation for its application in high-temperature reaction systems. The results validated that Cu-BTC, functioning as an enzyme-like biomimetic catalyst, offered distinct advantages in catalytic systems that require elevated temperature conditions.

Based on the analysis of the relevant literature,<sup>22</sup> it can be inferred that the metallic group of Cu-BTC involves a pair of Cu<sup>2+</sup> ions coordinated by four carboxylate bridges to form a paddle-wheel moiety. The central Cu<sup>2+</sup> in the framework structure adopts a coordination number of 6, with three Cu<sup>2+</sup> ions spatially coordinated to the 12 O atoms from the 6 carboxyl groups of 2 organic ligands, BTC. Axially, it coordinates with two water molecules, as illustrated in Fig. 4.

### 3.2 Evaluation of PPO mimetic activity of Cu-BTC

**3.2.1 Optimization of Cu-BTC PPO mimetic activity.** PPO can catalyse the oxidation of simple phenolic compounds to form quinones, with the resulting products exhibiting a maximum absorption peak at a wavelength of 420 nm.<sup>23</sup> The absorbance value is positively correlated with the amount of product generated, making it a common method for measuring the enzyme activity of PPO. In this study, catechol was used as the substrate to observe the colour changes after the addition of a chromogenic system and to determine the

UV-vis absorption spectrum, thereby verifying the PPO-like enzyme activity of Cu-BTC. The results indicated that after the addition of Cu-BTC to the chromogenic system and a specified period of water bath heating, the colour transitioned from light blue in the control group to yellow in the Cu-BTC group. The UV-vis absorption spectra demonstrated that following the colour reaction, the absorption peak at 270 nm significantly decreased, while a new absorption peak emerged around 410 nm, as illustrated in Fig. 5(a). The above results clearly validate the intrinsic PPO-like activity of the prepared Cu-BTC.

To further investigate the PPO-like activity of the synthesized Cu-BTC and to optimize its synthesis conditions, this study also examined the effects of pH, reaction temperature, time, and Cu-BTC dosage on the polyphenol oxidase-like activity of Cu-BTC, as illustrated in Fig. 5(b)–(e). As the reaction temperature increased, the enzyme-like activity of Cu-BTC initially rose and then declined, peaking at 70 °C. The optimal reaction temperature for Cu-BTC was significantly higher than that for polyphenol oxidase (approximately 30 °C), indicating that Cu-BTC exhibits markedly superior thermal stability compared to polyphenol oxidase. When the pH increased from 3.5 to 5.0, the catalytic activity of Cu-BTC sharply increased, reaching its peak at pH 5.0, which was 2.5 times the enzyme activity observed at pH 3.5. Subsequently, as the pH continued to rise, the enzymatic activity of Cu-BTC exhibited a declining trend. The enzyme-like activity of Cu-BTC demonstrates a concentration dependency. When the dosage of Cu-BTC is below 0.01 g mL<sup>-1</sup>, the enzyme activity rapidly increases with rising Cu-BTC dosage. Conversely, when the dosage exceeds 0.01 g mL<sup>-1</sup>, the enzyme activity fluctuates within a specific range. Additionally, the enzyme-like activity of Cu-BTC exhibits a time dependency, with the catalytic activity reaching its maximum within 10 minutes.

Similar to natural PPO, Cu-BTC features a three-dimensional structure formed by two copper ions (Cu<sup>2+</sup>) coordinated with four carboxylate groups, wherein the dinuclear copper active site serves as the primary functional centre of the nanoenzyme.<sup>24</sup> Consequently, Cu-BTC exhibits catalytic activity that parallels that of PPO, with its performance being influenced by external environmental factors such as temperature and pH. Typically, it demonstrates maximum activity within a specific range, exhibiting a declining trend in activity when conditions fall outside this range. These variations can be attributed to the stability of the active centre and the electrostatic interactions between the metal-organic framework (MOF) surface, substrate, and solvent molecules.<sup>25</sup> For example, when the reaction pH is less than 3, the strongly acidic environment may lead to the dissociation of copper ions from the MOF, thereby diminishing enzyme activity and causing irreversible inactivation.<sup>26</sup> Conversely, when the pH exceeds the optimal level, the MOF surface tends to acquire a negative charge, which repels and obstructs anionic molecules from approaching the MOF surface, ultimately resulting in a decrease in its catalytic activity.

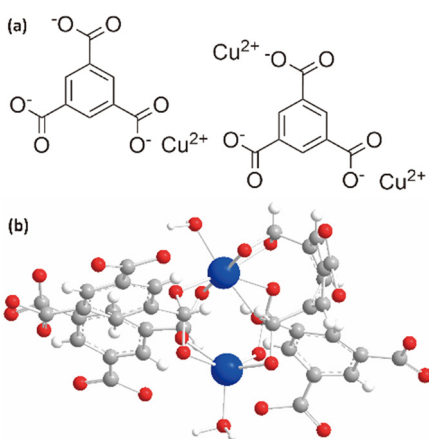


Fig. 4 (a) Structure representation of Cu-BTC and (b) sketch of the main structure of Cu-BTC.



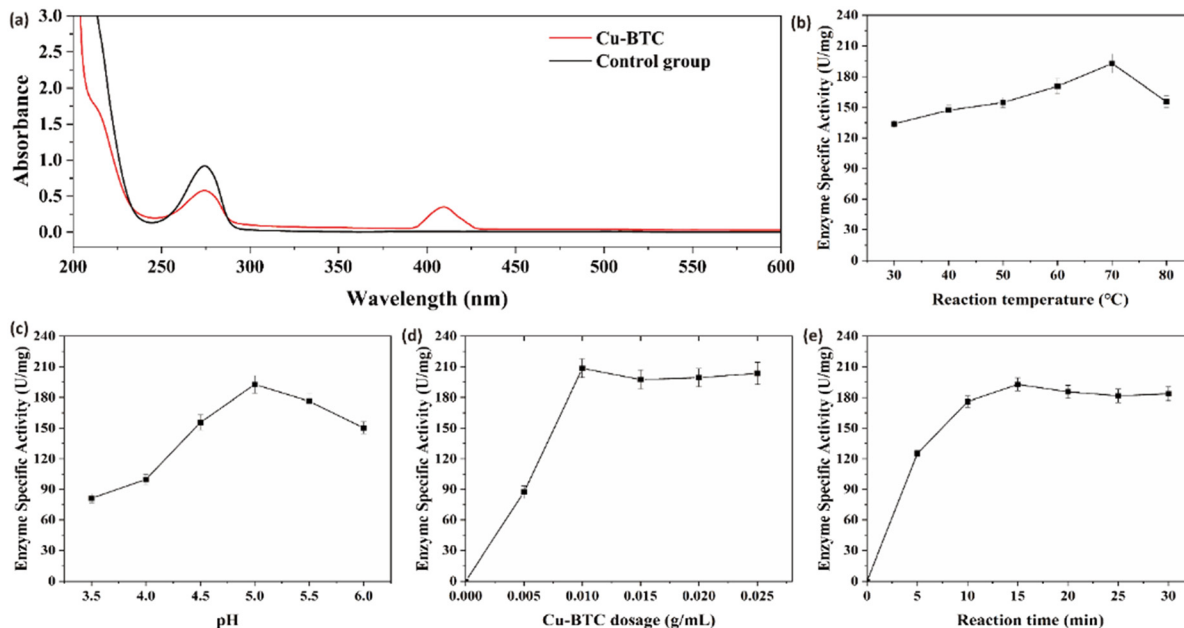


Fig. 5 (a) UV-vis absorption spectra of catechins using Cu-BTC; effects of synthesis conditions on the enzyme-like activity of Cu-BTC: (b) reaction temperature; (c) pH; (d) Cu-BTC dosage; (e) reaction time.

Based on this analysis, the optimal reaction conditions for determining Cu-BTC using the catechol method are as follows: a reaction temperature of 70 °C, a pH of 5.0, a Cu-BTC dosage of 0.01 g mL<sup>-1</sup>, and a reaction time of 10 minutes, achieving the highest enzyme activity of 200 U mg<sup>-1</sup>.

**3.2.2 Enzyme kinetics study of Cu-BTC.** The enzymatic reaction kinetics of Cu-BTC were investigated by varying the concentration of catechol. Under consistent experimental conditions (pH = 5, Cu-BTC dosage of 0.1 g mL<sup>-1</sup>, reaction time of 15 minutes, and reaction temperature of 70 °C), the influence of catechol concentration on the rate of the enzymatic oxidation reaction was examined, with the results presented in Fig. 6(a). The initial reaction rate ( $v$ ) of the enzymatic reaction increased with the rise in substrate catechol concentration ( $c$ ), and the relationship between  $v^{-1}$  and  $c^{-1}$  exhibited linearity, indicating that the enzymatic reaction kinetics of Cu-BTC adhere to the typical Michaelis-Menten equation.

$$v = \frac{v_{\max}c}{(K_m + c)}$$

Here,  $v$  represents the initial reaction rate (mM s<sup>-1</sup>),  $v_{\max}$  denotes the maximum reaction rate (mM s<sup>-1</sup>), and  $K_m$  is the Michaelis constant (mM).

The Michaelis constant ( $K_m$ ) represents the substrate concentration at which the enzyme-catalyzed reaction achieves half of its maximum velocity ( $v_{\max}$ ), thereby reflecting the enzyme's affinity for various substrates. A smaller  $K_m$  value indicates a higher affinity of the enzyme for the substrate, increasing the likelihood that the enzyme-catalysed reaction will proceed.<sup>27</sup> The Hanes-Woolf plot method was utilized, and the results are illustrated in Fig. 6(b). Regression fitting yielded a Michaelis constant ( $K_m$ ) and a maximum reaction rate ( $v_{\max}$ ) of 14.19 mM and 0.0338 mM s<sup>-1</sup>, respectively, for the synthesized Cu-BTC. These findings confirm that Cu-BTC has a Michaelis constant ( $K_m$ )

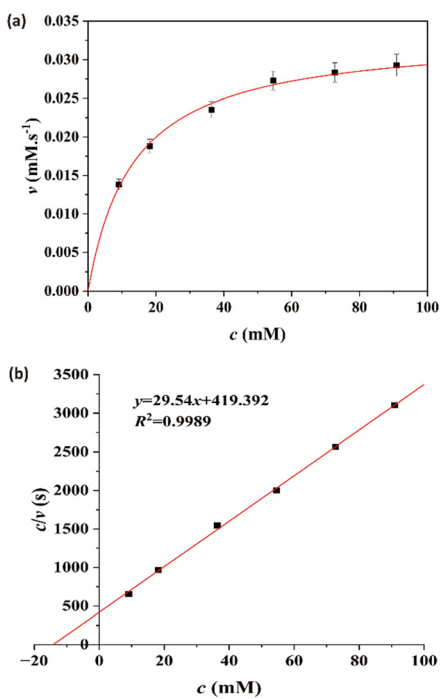


Fig. 6 (a) Michaelis-Menten plot of the Cu-BTC enzyme-like activity; (b) Hanes-Woolf plot of the Cu-BTC enzyme-like activity.



comparable to that of tea isoenzymes, demonstrating significant enzyme-like activity.<sup>28</sup>

### 3.3 Bionic catalytic synthesis of theaflavins

From the enzyme activity experiment, it was determined that Cu-BTC exhibits polyphenol oxidase-like catalytic activity, enabling it to oxidize catechol to *o*-benzoquinone. This reaction is also the key process catalyzed by polyphenol oxidase in the oxidative polymerization of catechins to synthesize theaflavins. To assess the feasibility of using Cu-BTC in the synthesis of theaflavins, we employed mixed catechins as the reaction substrate and compared the yields of theaflavins synthesized using Cu-BTC with those obtained through various chemical oxidation methods (ferric nitrate, ferric sulfate, ferric chloride, hydrogen peroxide, potassium permanganate, and ammonia) and tyrosinase catalysis. The results, illustrated in Fig. 7, indicate that the total yield of theaflavins produced *via* Cu-BTC biomimetic catalysis is at least 30% higher than that achieved through chemical oxidation and 50% higher than that obtained using the tyrosinase method. This finding suggests that Cu-BTC demonstrates strong catalytic activity and offers an efficient, low-cost alternative for the synthesis of theaflavins.

To optimize the biomimetic catalysis of Cu-BTC, single-factor experiments were conducted on reaction temperature,

pH, reaction time, and Cu-BTC dosage, with the results illustrated in Fig. 8.

Under the conditions of a reaction time of 60 minutes, a pH of 5.0, and a Cu-BTC dosage of 0.05 g mL<sup>-1</sup>, the yield of theaflavin was investigated at reaction temperatures ranging from 60 to 90 °C, as presented in Fig. 8(b). As shown in Fig. 8(b), the reaction temperature significantly influences the synthesis of theaflavin. Below 80 °C, the yield of theaflavin increases rapidly with rising temperature, with the yield at 80 °C being twice that at 60 °C. However, when the temperature exceeds 80 °C, the yield of theaflavin decreases, which may be attributed to the reduced solubility of oxygen at elevated temperatures.<sup>29</sup>

Like other nanomaterial-based nanozymes, Cu-BTC is also influenced by pH.<sup>30</sup> The effect of pH on the yield of theaflavin was investigated over a range of 3 to 8, under the conditions of a reaction time of 60 minutes, a Cu-BTC dosage of 0.05 g mL<sup>-1</sup>, and a temperature of 80 °C, as illustrated in Fig. 8(d). The results confirmed that pH significantly impacts the yield of theaflavin. When the pH is below 5, the catalytic activity of Cu-BTC increases with rising pH, leading to an enhanced yield of the total theaflavin. However, when the pH exceeds 5, the yield of the total theaflavin decreases. Therefore, the optimal catalytic activity of Cu-BTC occurs at pH = 5. Research indicated that the morphology and structure of Cu-MOF are influenced by pH levels, resulting in variations in the number of exposed active sites on its surface, which, in turn, affects its catalytic activity.<sup>31</sup>

At pH 5.0, with a Cu-BTC dosage of 0.05 g mL<sup>-1</sup> and a temperature of 80 °C, the variation in the total theaflavin yield with reaction time was monitored, and the results are presented in Fig. 8(f). The findings indicated that the biomimetic catalytic reaction of theaflavin reaches its maximum yield within 60 minutes, and extending the reaction time beyond this point does not result in an increased yield. This phenomenon is likely due to the gradual consumption of the substrate, catechins, which reaches equilibrium at 60 minutes; thus, the optimal reaction time was determined to be 60 minutes.

At pH 5.0, with a reaction time of 60 minutes and a temperature of 80 °C, the total theaflavin yield was compared across Cu-BTC dosages ranging from 0.01 g mL<sup>-1</sup> to 0.1 g mL<sup>-1</sup> (Fig. 8(h)). When the dosage of Cu-BTC is below 0.05 g mL<sup>-1</sup>, the yield of theaflavins exhibited a dose-dependent relationship. However, when the dosage exceeds 0.05 g mL<sup>-1</sup>, the yield of theaflavins showed minimal variation. This may be attributed to the fact that a higher dosage of Cu-BTC leads to an increased reaction rate, resulting in a shorter time required to achieve reaction equilibrium. Conversely, when the dosage is less than 0.05 g mL<sup>-1</sup>, the time required to reach equilibrium exceeds 60 minutes. Therefore, at the 60 minute mark, the reaction has not yet reached equilibrium, which results in a lower yield of the total theaflavins.

As illustrated in Fig. 8(a), the Cu-BTC biomimetic catalytic method demonstrates a significant advantage in the yields of TF1 and TFDG among the four major theaflavins, in contrast to TF2A and TF2B. Notably, TF1 displays the greatest fluctuation

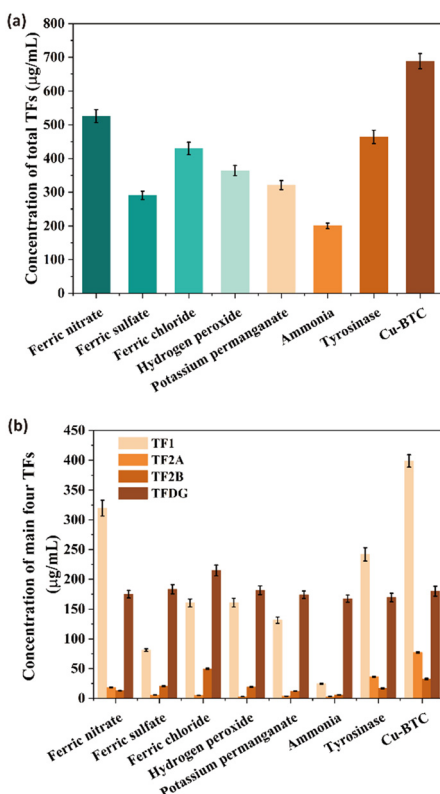
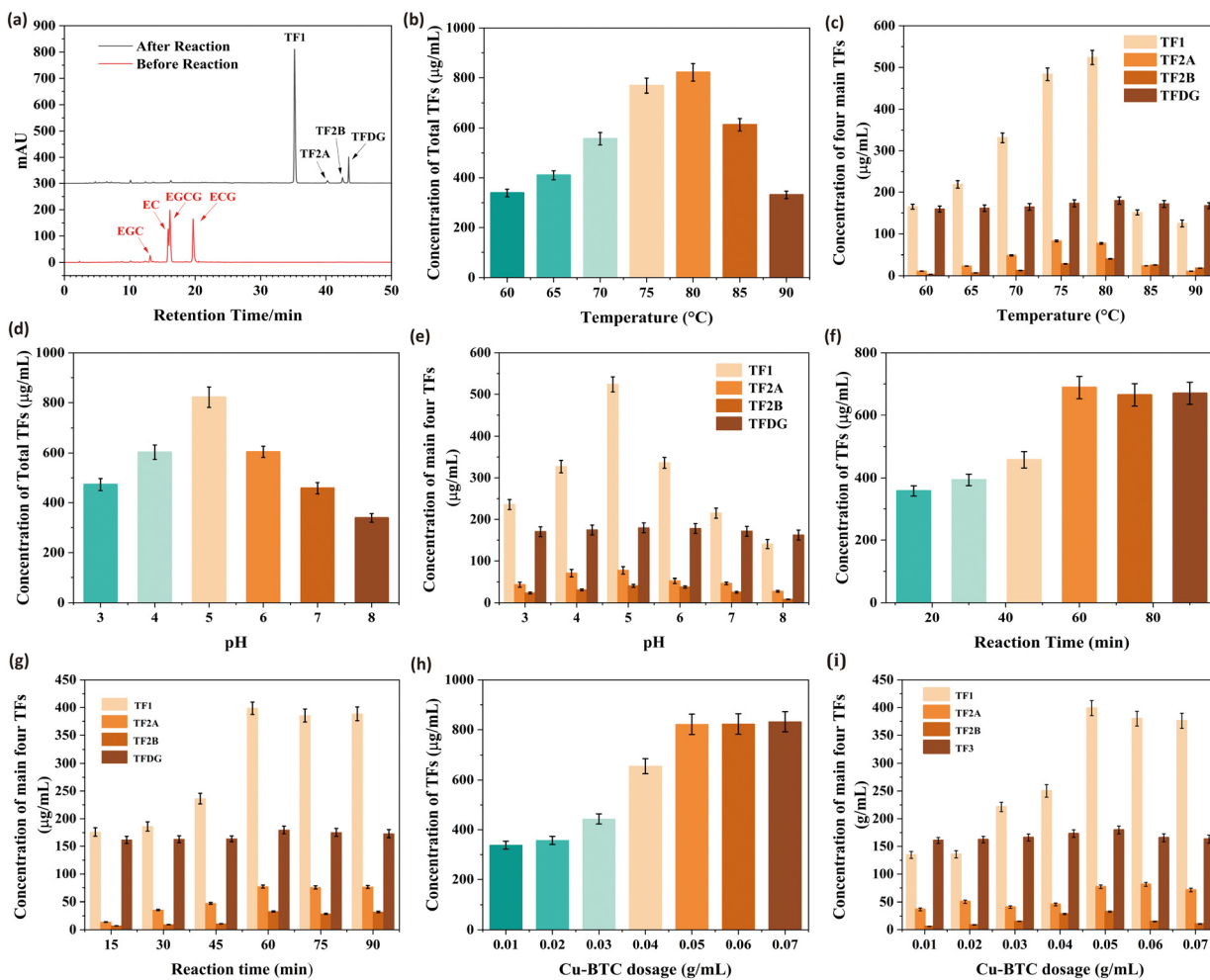


Fig. 7 Comparison of the (a) concentration of total TFs and (b) concentration of four main TFs using different synthesis methods.





**Fig. 8** (a) HPLC chromatogram profiles before and after the bionic catalytic synthesis of TFs; effects of (b) and (c) reaction temperature, (d) and (e) pH, (f) and (g) reaction time and (h) and (i) proportion of Cu-BTC/catechins on the concentration of total TFs and concentration of four main TFs.

in yield under the specified reaction conditions. This observation may be attributed to the substrate selectivity of Cu-BTC, which preferentially catalyses the synthesis of TFDG under these conditions. Fig. 8(c), (e), (g), and (i) validate that it is possible to use PPOs as catalysts for commercial-scale production of individual theaflavin components.

## 4. Conclusions

In summary, using copper nitrate ( $\text{Cu}(\text{NO}_3)_2$ ) as the copper source and benzene-1,3,5-tricarboxylic acid ( $\text{H}_3\text{BTC}$ ) as the ligand, we prepared the copper-based organic framework Cu-BTC *via* a hydrothermal method. The obtained octahedral MOF microcrystals exhibited excellent PPO-like enzyme activity and demonstrated better thermal stability and catalytic efficiency than natural enzymes. Incorporating Cu-BTC into catechins could achieve a higher total theaflavin conversion rate compared to chemical oxidation methods and tyrosinase. The optimal reaction conditions for the Cu-BTC biomimetic catalytic oxidation of catechins to synthesize theaflavins were as follows: a reaction temperature of 80 °C,

a pH of 5.0, a Cu-BTC dosage of 0.05 g  $\text{mL}^{-1}$ , and a reaction time of 60 minutes, with a corresponding total theaflavin conversion rate of 800  $\mu\text{g mL}^{-1}$ . Compared to natural enzymes, the Cu-BTC mimic enzyme is simpler to prepare, more cost-effective, and has broader reaction conditions, offering a new, low-cost, and high-efficiency synthetic approach beyond existing enzymatic oxidation methods.

## Author contributions

SD: conceptualization, methodology, resources, investigation, writing – review & editing and funding acquisition; ZZ: supervision and project administration; ZD: data curation, writing – review & editing; JC: investigation, formal analysis, and writing – original draft.

## Conflicts of interest

The authors declare that they have no known competing financial interests or personal relationships that could have appeared to influence the work reported in this paper.

## Data availability

All relevant data are within the paper.

## Acknowledgements

The authors gratefully acknowledge the funding and support provided by the Hunan Provincial Natural Science Foundation of China grant: No. 2023JJ50034.

## Notes and references

- 1 S. L. Du, J. Y. Chang and Z. M. Zhou, A comprehensive review of theaflavins: Physiological activities, synthesis techniques, and future challenges, *Food Sci. Nutr.*, 2025, **13**(8), e70762, DOI: [10.1002/fsn3.70762](https://doi.org/10.1002/fsn3.70762).
- 2 T. Negi, Y. Kumar, R. Sirohi, S. Singh, A. Tarafdar, S. Pareek, M. K. Awasthi and N. A. Sagar, Advances in bioconversion of spent tea leaves to value-added products, *Bioresour. Technol.*, 2022, **346**, 126409, DOI: [10.1016/j.biortech.2021.126409](https://doi.org/10.1016/j.biortech.2021.126409).
- 3 J. H. Ye, Y. Ye, J. F. Yin, J. Jin, Y. R. Liang, R. Y. Liu, P. Tang and Y. Q. Xu, Bitterness and astringency of tea leaves and products: Formation mechanism and reducing strategies, *Trends Food Sci. Technol.*, 2022, **123**, 130–143, DOI: [10.1016/j.tifs.2022.02.031](https://doi.org/10.1016/j.tifs.2022.02.031).
- 4 H. Zhao, L. Zhu and Y. Wang, Theaflavins with health-promoting properties: From extraction, synthesis to medicinal application, *Trends Food Sci. Technol.*, 2025, **155**, 104804, DOI: [10.1016/j.tifs.2024.104804](https://doi.org/10.1016/j.tifs.2024.104804).
- 5 Y. Liu, D. Wang, J. Li, Z. Zhang, Y. Wang, C. Qiu, Y. Sun and C. Pan, Research progress on the functions and biosynthesis of theaflavins, *Food Chem.*, 2024, **450**, 139285, DOI: [10.1016/j.foodchem.2024.139285](https://doi.org/10.1016/j.foodchem.2024.139285).
- 6 S. Sur and C. K. Panda, Molecular aspects of cancer chemopreventive and therapeutic efficacies of tea and tea polyphenols, *Nutrition*, 2017, **43–44**, 8–15, DOI: [10.1016/j.nut.2017.06.006](https://doi.org/10.1016/j.nut.2017.06.006).
- 7 J. Jian, J. An, Z. Gao, L. Zeng, W. Luo and Y. Ding, The enzymatic synthesis of theaflavin-3-gallate oxidation product and its determination, *Talanta*, 2024, **276**, 126239, DOI: [10.1016/j.talanta.2024.126239](https://doi.org/10.1016/j.talanta.2024.126239).
- 8 H. Zou, Q. Xiao, G. Li, X. Wei, X. Tian, L. Zhu, F. Ma and M. Li, Revisiting the advancements in plant polyphenol oxidases research, *Sci. Hortic.*, 2025, **341**, 113960, DOI: [10.1016/j.scienta.2025.113960](https://doi.org/10.1016/j.scienta.2025.113960).
- 9 O. S. Aloo, D. G. Kim, S. Vijayalakshmi, D. O. Aloo, C. O. Ochola and D. H. Oh, Polyphenol constituents and impacts of fermented teas (*Camellia sinensis*) in human wellness, *Food Biosci.*, 2024, **60**, 104389, DOI: [10.1016/j.fbio.2024.104389](https://doi.org/10.1016/j.fbio.2024.104389).
- 10 D. Panadare and V. K. Rathod, Extraction and purification of polyphenol oxidase: A review, *Biocatal. Agric. Biotechnol.*, 2018, **14**, 431–437, DOI: [10.1016/j.biab.2018.03.010](https://doi.org/10.1016/j.biab.2018.03.010).
- 11 Y. Li, H. Chai, Z. Yuan, C. Huang, S. Wang, Y. Sun, X. Zhang and G. Zhang, Metal-organic framework-engineered enzyme/nanozyme composites: Preparation, functionality, and sensing mechanisms, *Chem. Eng. J.*, 2024, **496**, 153884, DOI: [10.1016/j.cej.2024.153884](https://doi.org/10.1016/j.cej.2024.153884).
- 12 M. Wang, X. Zhou, Y. Li, Y. Dong, J. Meng, S. Zhang, L. Xia, Z. He, L. Ren, Z. Chen and X. Zhang, Triple-synergistic MOF-nanozyme for efficient antibacterial treatment, *Bioact. Mater.*, 2022, **17**, 289–299, DOI: [10.1016/j.bioactmat.2022.01.036](https://doi.org/10.1016/j.bioactmat.2022.01.036).
- 13 M. Yang, N. Wang, X. Wang, R. Zhang, I. N. Etim, M. E. Yue, J. Duan, B. Hou and W. Sand, Construction of CeO<sub>2</sub>-MOF nanorods with oxygen vacancies for nanozyme catalytic antibacterial application, *J. Ind. Eng. Chem.*, 2025, **149**, 554–565, DOI: [10.1016/j.jiec.2025.02.015](https://doi.org/10.1016/j.jiec.2025.02.015).
- 14 Q. Y. Yang, C. Q. Wan, Y. X. Wang, X. F. Shen and Y. H. Pang, Bismuth-based metal-organic framework peroxidase-mimic nanozyme: Preparation and mechanism for colorimetric-converted ultra-trace electrochemical sensing of chromium ion, *J. Hazard. Mater.*, 2023, **451**, 131148, DOI: [10.1016/j.jhazmat.2023.131148](https://doi.org/10.1016/j.jhazmat.2023.131148).
- 15 J. Xiong, X. Yuan, Z. Li, M. H. Zong, W. Y. Lou and X. Wu, Insights into Amorphous Metal-Organic Framework as Carbonic Anhydrase Mimic, *ChemCatChem*, 2024, **16**, e202400356, DOI: [10.1002/cctc.202400356](https://doi.org/10.1002/cctc.202400356).
- 16 A. K. Singh, D. Sharma, D. K. Singh, S. Sarraf, A. K. Basu, V. Ganesan, A. Saha and A. Indra, Oxidase-Like Nanozyme Activity of Ultrathin Copper Metal-Organic Framework Nanosheets With High Specificity for Catechol Oxidation, *ChemCatChem*, 2024, **17**, e202401029, DOI: [10.1002/cctc.202401029](https://doi.org/10.1002/cctc.202401029).
- 17 A. A. Ibrahim, M. M. Kaid, S. L. Ali, S. E. Samra, S. A. El-Hakam and A. I. Ahmed, Applications of nanostructure phosphomolybdic acid/strontium MOF for removal of Rhodamine B and synthesis of pharmaceutically significant 14-Aryl-14-alkyl-14-H-dibenzoxanthene and 7-hydroxy-4-methyl coumarin, *Inorg. Chem. Commun.*, 2023, **153**, 110748, DOI: [10.1016/j.inoche.2023.110748](https://doi.org/10.1016/j.inoche.2023.110748).
- 18 K. Zhan, Z. L. Yang, Z. Y. Xu, Z. F. Lai, J. Li, L. J. Chen, S. X. Zhou, M. X. Li and Y. D. Gan, Comparison of Soluble and Membrane-Bound Polyphenol Oxidase Characteristics of Tea Cultivars Suitable for Making Ninghong Black Tea, *Chaye Kexue*, 2023, **43**(3), 356–366, DOI: [10.13305/j.cnki.jts.2023.03.003](https://doi.org/10.13305/j.cnki.jts.2023.03.003).
- 19 X. Kong, W. Xu, K. Zhang, G. Chen and X. Zeng, Effects of reaction temperature, pH and duration on conversion of tea catechins and formation of theaflavins and theasinsins, *Food Biosci.*, 2023, **54**, 102911, DOI: [10.1016/j.fbio.2023.102911](https://doi.org/10.1016/j.fbio.2023.102911).
- 20 J. Y. Zhang, H. Y. Jiang, H. C. Cui and Y. W. Jiang, Study on Affecting Factors and Factors Model of the Theaflavins Acidity Oxidation Formation, *Shipin Yanjiu Yu Kaifa*, 2011, **32**(8), 1–4+61, DOI: [10.3969/j.issn.1005-6521.2011.08.001](https://doi.org/10.3969/j.issn.1005-6521.2011.08.001).
- 21 J. Y. Zhang, H. Y. Jiang, H. C. Cui and Y. W. Jiang, Mechanism of the Influence of Catechin Composition on the Formation of Theaflavins by Chemical Oxidation, *Shipin Gongye Keji*, 2011, **32**(12), 85–89+92, DOI: [10.13386/j.issn1002-0306.2011.12.133](https://doi.org/10.13386/j.issn1002-0306.2011.12.133).
- 22 M. Todaro, G. Buscarino, L. Sciortino, A. Alessi, F. Messina, M. Taddei, M. Ranocchiari, M. Cannas and F. M. Gelardi,



Decomposition process of carboxylate MOF HKUST-1 unveiled at the atomic scale level, *J. Phys. Chem. C*, 2016, **120**(23), 12879–12889, DOI: [10.1021/acs.jpcc.6b03237](https://doi.org/10.1021/acs.jpcc.6b03237).

23 J. Li, Z. Y. Deng, H. H. Dong, R. Tsao and X. R. Liu, Substrate specificity of polyphenol oxidase and its selectivity towards polyphenols: Unlocking the browning mechanism of fresh lotus root (*Nelumbo nucifera* Gaertn.), *Food Chem.*, 2023, **424**, 136392, DOI: [10.1016/j.foodchem.2023.136392](https://doi.org/10.1016/j.foodchem.2023.136392).

24 S. Roy, J. Darabdhara and M. Ahmaruzzaman, Recent advances of Copper-BTC metal-organic frameworks for efficient degradation of organic dye-polluted wastewater: Synthesis, mechanistic insights and future outlook, *J. Hazard. Mater. Lett.*, 2024, **5**, 100094, DOI: [10.1016/j.hazl.2023.100094](https://doi.org/10.1016/j.hazl.2023.100094).

25 N. B. Patel, N. Vala, A. Shukla, S. Neogi and M. K. Mishra, Catalytic activity of Cu-BTC metal organic framework for borrowing hydrogen and tandem reactions of an alcohol under solvent and base free condition, *Inorg. Chim. Acta*, 2023, **554**, 121546, DOI: [10.1016/j.ica.2023.121546](https://doi.org/10.1016/j.ica.2023.121546).

26 N. P. S. Chauhan, P. Perumal, N. S. Chundawat and S. Jadoun, Achiral and chiral metal-organic frameworks (MOFs) as an efficient catalyst for organic synthesis, *Coord. Chem. Rev.*, 2025, **533**, 216536, DOI: [10.1016/j.ccr.2025.216536](https://doi.org/10.1016/j.ccr.2025.216536).

27 C. Mbira, Influence of substrate concentration on enzyme activity in bio catalysis, *J. Chem.*, 2024, **3**(1), 48–58, DOI: [10.47672/jchem.1976](https://doi.org/10.47672/jchem.1976).

28 J. Teng, Isolation and identification of polyphenol oxidase isozymes from *Camellia sinensis* and its enzymatic synthesis of theaflavins, [Master's Thesis], Hunan Agricultural University, Changsha, 2015.

29 X. Liu, P. An, Y. Han, H. Meng and X. Zhang, MOF-818(Cu)-derived bi-nanozymes of laccase and catecholase mimics and colorimetric sensing to epinephrine, *Microchem. J.*, 2024, **201**, 110559, DOI: [10.1016/j.microc.2024.110559](https://doi.org/10.1016/j.microc.2024.110559).

30 Y. Yang, G. Q. Liu, S. L. Yang, X. L. Ai, Q. H. Liang, L. P. Luo, R. Wang, J. L. Wang and W. B. Zhang, Study on a Colorimetric Method for the Detection of Ascorbic Acid in Fruit Juices Based on the Oxidase-like Activity of Ce-BDC, *Fenxi Ceshi Xuebao*, 2021, **40**(5), 678–683, DOI: [10.3969/j.issn.1004-4957.2021.05.00](https://doi.org/10.3969/j.issn.1004-4957.2021.05.00).

31 Y. Zhang, S. Wang, B. B. Chen and Y. Fu, Influence of the pH of acetic acid aqueous solution on the morphological and structural reversible transformation of Cu-BDC, *Huagong Xinxing Cailiao*, 2023, **51**(5), 128–133, DOI: [10.19817/j.cnki.issn1006-3536.2023.05.023](https://doi.org/10.19817/j.cnki.issn1006-3536.2023.05.023).

